Biochimica et Biophysica Acta, 944 (1988) 164–176
Elsevier

BBA 74137

The effect of potential-sensitive molecular probes on the thermal phase transition in dimyristoylphosphatidyl choline preparations

J. Fumero, B.P. Bammel, H.P. Hopkins and J.C. Smith

Department of Chemistry and Laboratory for Microbial and Biochemical Sciences, Georgia State University, Atlanta, GA (U.S.A.)

(Received 14 January 1988)
(Revised manuscript received 24 June 1988)

Key words: Molecular probe; Calorimetry; Phospholipid; Bilayer

Differential scanning calorimetry (DSC) has been employed to determine the effect of five commonly employed extrinsic potential-sensitive probes on phase transitions of multilamellar suspensions of L-α-dimyristoylphosphatidylcholine (DMPC). At mol% values of less than five, the effect of these probes on the excess heat capacity curve in the vicinity of the gel to liquid crystal phase transition can be described by an equation based on the formation of ideal solutions in both phases. Even at up to 4 mol%, these dyes only moderately reduce the enthalpy change associated with this transition, but cause a marked decrease in the size of the cooperative unit parameter. The excess heat capacity profile for diS-C_3-(5) is represented by the ideal solution equation, even at 12 mol%, whereas the suspensions with the other probes present at this level have profiles covering large temperature ranges. Multiple peaks appear at the higher levels for the negatively charged oxonols V and VI, and merocyanine 540, a result consistent with the presence of well-defined microdomains or even phase separation. The enthalpy change associated with the transition near 15 °C involving packing in the headgroup region is decreased significantly, indicating that the probes probably affect the lipid headgroup conformation, even at low levels. The cyanine probe diS-C_3-(5) causes the heat capacity profile of small unilamellar vesicles to be transformed very rapidly into one similar to that of the vortexed lipid preparations, presumably by a dye-mediated vesicle fusion process, enhanced by the surface location of this probe. All our results are consistent with diS-C_3-(5) being located on the surface of the bilayer in both phases, but a penetration of the other probes into the hydrocarbon region, at least in the liquid crystal phase.

Introduction

Dyes belonging to the polyene class have often proved to be useful as extrinsic indicators of charge separation and associated electrical potential gradient across membranes in diverse biological preparations [1–6]. The efficacy of this techniques

Abbreviations: DSC, differential scanning calorimetry; DMPC, L-α-dimyristoylphosphatidylcholine; CUP, cooperative unit parameter.

Correspondence: H.P. Hopkins or J.C. Smith, Department of Chemistry and Laboratory of Microbial and Biochemical Sciences, Georgia State University, Atlanta, GA 30303, U.S.A.

depends in part on the location of the potential-sensitive probes in the membrane bilayer, and the extent to which these probes interact with the membrane and alter its structure. In multilamellar preparations (models for membranes), which can be formed by vortexing pure lipids in a buffer, the lipid molecules form bilayers and often exist in a highly ordered state (hydrocarbon chains in an all-*trans*, linear configuration) below a given temperature (T_m), called the gel-to-liquid crystal transition temperature [7–10]. When the suspensions are heated, e.g., in a high-sensitivity differential scanning calorimeter (DSC), the lipids undergo a transition to a disordered, but still bilayer, state. Analysis of the calorimetric data yields the temperature at the midpoint of the transition (T_m), the total enthalpy change for the transition (ΔH_{cal}), and the cooperative unit parameter (CUP). As a part of a series of investigations designed to address the probe location issue, these parameters for the gel-to-liquid crystal transition and also those for the pretransition, thought to involve the orientation of headgroups [9], were monitored for preparations of L-α-dimyristoylphosphatidylcholine (DMPC) as a function of the mole fraction of a number of commonly employed potential-sensitive molecular probes (Fig. 1).

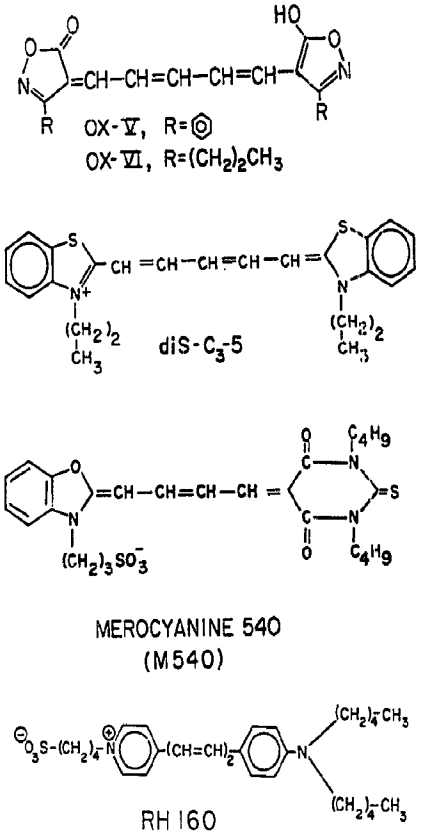

Fig. 1. The structure of the probes employed in this investigation. The hydroxyl group proton in the oxonol V and VI compounds has a pK_a of approx. 4; these two probes thus exist as symmetrical anions under the experimental conditions employed in the present investigations.

Materials and Methods

High purity (above 99%) synthetic L-α-dimyristoylphosphatidylcholine was purchased from Avanti Polar Lipids, Birmingham, AL. Oxonols V and VI were synthesized according to the method described by Smith et al. [12]; diS-C_3-(5) was either the generous gift of Professor A. Waggoner or was purchased from Molecular Probes, Eugene, OR; this company also supplied RH 160. Merocyanine 540 was supplied by Eastman Kodak Co. KCl was supplied by Fisher Scientific Co. and all other materials were purchased from Sigma Chemical Co., St. Louis, MO. Each chemical was used as supplied and without further purification.

All calorimetric investigations were performed on multilamellar samples prepared by vortexing (Scientific Industries Vortex Jr. mixer) DMPC suspended in a medium consisting of 160 mM KCl, 0.1 mM EDTA and 10 mM Na-Hepes or phosphate buffer at pH 7.2. 10 ml of the suspension was vortexed until no lipid particles were visible, nominally 5 min, and the sample was then vortexed as vigorously as possible for another 15 min. This suspension was stirred over night at 40 °C using a magnetic stirrer and a teflon-coated stirrer bar. The sample was again vigorously vortexed for approx. 5 min before extracting an aliquot for dilution with buffer to the final lipid concentration of 2.5 mg/ml. All vortexing was performed at room temperature. The calorimetric properties of these vortexed samples were found to be extremely reproducibles. When dyes in solid form were added directly to the previously vortexed suspensions and the samples were then stirred for a minimum of 12 h at 40 °C, multiple peaks were not observed in the calorimetric profiles at mol% values less than 3.

At mol% values greater than 3, the lipid and probes were dissolved in chloroform and this mixture was used to form a thin film on the surface of a 25-ml round-bottom flask. The film was formed by passing nitrogen over the liquid mixture while swirling the flask. All remaining solvent was removed by placing the samples in a vacuum for 12 h. Suspensions were then formed with these films as previously described.

Small unilamellar DMPC vesicles were prepared by a sonication procedure described by Bammel et al. [11]. Final lipid concentrations (8–10 mM) for a stock vesicle suspensions were derived from a colorimetric phosphate determination procedure [18], and the size distribution was determined by electron microscopy.

All calorimetric experiments were performed with an MC-2 differential scanning calorimeter purchased from Microcal, Inc. Both the temperature and power signals were recorded digitally and these data were transformed into the excess heat capacity profiles by programs supplied by Microcal, Inc. In repeated measurements on a suspension with 2.5 mg lipid per ml, the temperature values at the peak of the transition could be reproduced to $\pm 0.02°C$, and the enthalpy determined from the numerical integration of the area under the excess heat capacity curve could be reproduced to within 0.05 kcal/mol. However, because of the sharpness of the gel-to-liquid crystal phase transition for DMPC, only with a scan rate of 6°C per h could we measure accurately the top portion of the narrow peak and thus determine accurately the ΔH_{cal} and CUP values. When the dyes were present in the suspensions, the excess heat capacity profiles were much broader, and the data were taken at a scan rate of 45°C per h. A van 't Hoff enthalpy change for the transition was calculated by the software supplied by Microcal from the equation

$$\Delta H_{vH} = 4RT_m^2 \Delta C_p(\max)/\Delta H_{cal} \quad (1)$$

which is based on the assumption that the phase transition can be described by a two-state model [13–15]. However, if the transition is highly cooperative such as the gel-to-liquid crystal transition, then this enthalpy change will be significantly larger than the calorimetric enthalpy. The accepted measure of this phenomenon is the cooperative unit parameter, CUP,

$$\text{CUP} = \Delta H_{vH}/\Delta H_{cal} \quad (2)$$

which was originally defined by Zimm and Bragg [16] for one-dimensional systems. It is not, however, as Kanehisa and Tsong [17] stated, to be equated explicitly to the number of lipids molecules or hydrocarbon chains undergoing the transition simultaneously, but is merely used as a measure of the cooperativity of the transitions.

Results

Calorimetric profiles for the vortexed DMPC suspensions exhibited a broad pretransition and sharp gel-to-liquid crystal transition, as can be seen in the unlabelled excess heat capacity curves shown in each of the panels of Figs. 2 and 5. The maxima in these curves were always found at 15.6 and 24.4°C, respectively; and the corresponding enthalpy changes (1.2 and 5.4 kcal/mol, respectively) and cooperative unit parameters (approx. 350 and 1200, respectively) are remarkably close to those reported by Dufour et al. [19] (T_m = 15.5 and 23.6°C; ΔH = 1.2 and 5.7 kcal/mol; CUP = 590 and 1300) and are similar to the parameters reported by others [20–22].

When any of the potential-sensitive probes shown in Fig. 1 were added to the vortexed suspension, only a single peak appeared at low mol% values but it was substantially broadened by the presence of dyes, even at mol% values near 0.5. The T_m moved only slightly to lower temperatures, and increasing the amount of dye up to three mol% caused no more than a 1°C decrease in T_m. In the range 3–4 mol%, the total width of the transition was nearer 1°C than the tenth of a degree observed for the pure lipid suspension. At mol% > 5, the transitions were so broad that the excess heat capacity curves could not easily be distinguished from the baseline when plotted on the same scale needed for the pure lipid. Such phenomena is readily apparent in the plots of the excess heat capacity at different mol% values shown in Fig. 2 for oxonol VI, merocyanine 540, diS-C_3-(5) and RH 160.

Three of the four types of probe included in this study cause ΔH_{cal} to decrease linearly as the

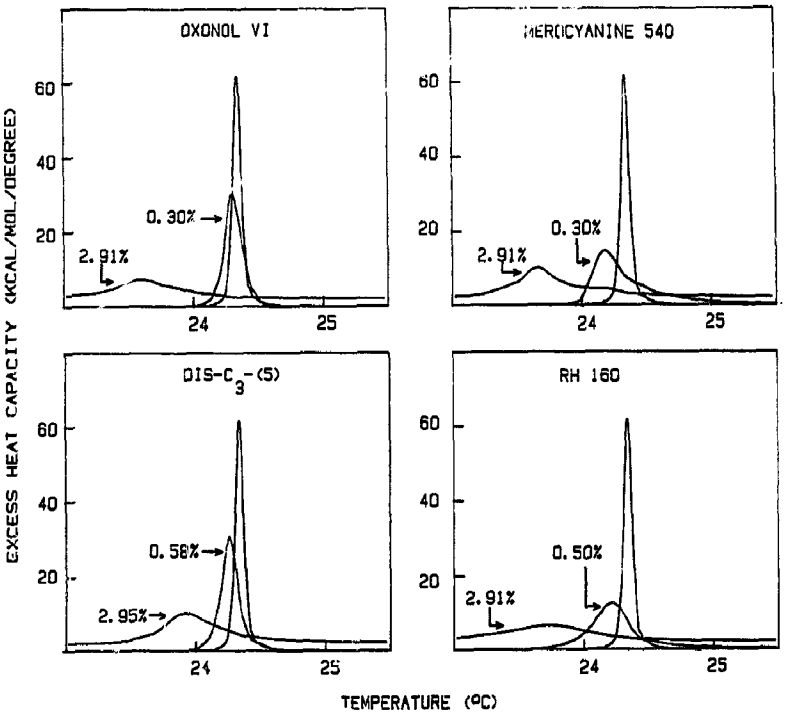

Fig. 2. Representative excess heat capacity profiles for suspensions of DMPC with merocyanine 540, diS-C_3-(5), oxonol VI and RH 160 at low probe-to-DMPC mol%. The sharpest profile shown in each panel is that of pure DMPC suspensions. The heat capacity scale has been set to zero for pure DMPC; each successive curve has been displaced upward for clarity.

mol% increased. Data for oxonol VI, merocyanine 540 and RH 160 are plotted in three panels of Fig. 3, and the lines shown are the least-squares fits. Similar effects were observed for oxonol V, but are not shown. In the presence of diS-C_3-(5), the profiles are broadened but the ΔH_{cal} determined from the area under the curve appears to be independent of concentration all the way up to 12 mol% (see lower left panel in Fig. 3). Notice that the line in each panel intersects the ordinate near 5.4, which is near the average (5455 ± 121 cal/mol) found by us in four independent investigations on pure suspensions of DMPC. This value is identical to that reported by Mabrey and Sturtevant [22], and we will use 5.4 kcal/mol in subsequent analyses.

Much larger effects are seen for the presence of the dyes on the cooperative unit parameter, as can be seen in the plots shown in the four panels shown in Fig. 4. All dyes reduce CUP to nearly 1/6 of that for the pure DMPC suspension at three mol%. At only 0.5 mol%, merocyanine 540 reduces CUP to the lowest value observed, yet the enthalpy for the transition has been only moderately affected. For all the probes except diS-C_3-(5), the maximum reduction in CUP is reached near 1 mol%, with only small changes at higher values. DiS-C_3-(5) also reduces the cooperativity of this transition, but the plateau is reached at 2 mol%.

All probes included in this study drastically affect the temperature and profile of the pretransition, and excess heat capacity curves presented in Fig. 5 are for the same probes for which profiles are shown in Fig. 2. For this transition, the probes lower the transition temperature more and cause greater broadening than that observed for the gel-to-liquid crystal transition. In the presence of all the probes, except diS-C_3-(5), the excess heat capacity profiles are too broad to be distinguished from the baseline at mol% > 3.

Enthalpy changes for the pretransition in the presence of four types of probe are shown as a function of mol% in Fig. 6. In contrast to the

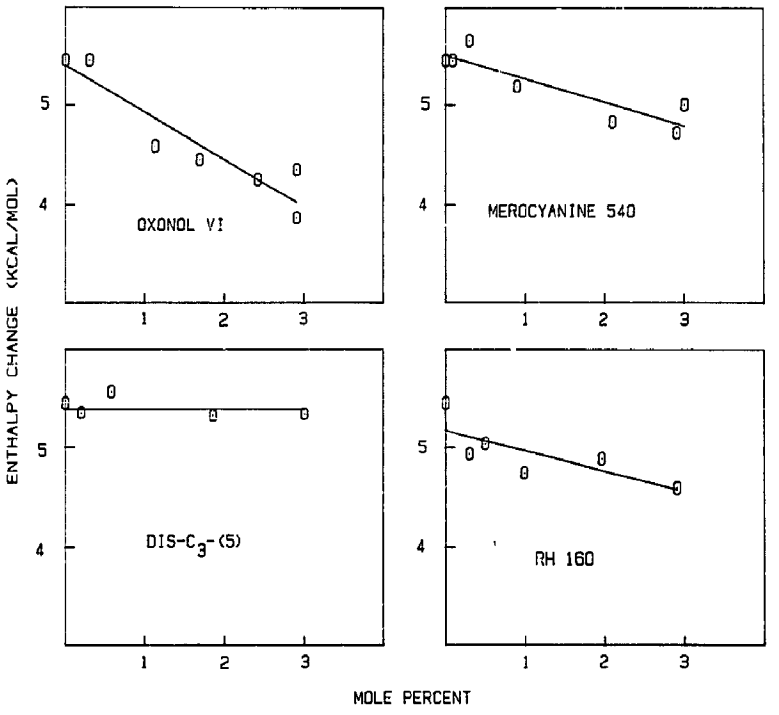

Fig. 3. The calorimetric enthalpy change for the main transition plotted as a function of the mol% values of the four types of probe used in this study. The lines are the linear least-squares fits for the data. Data for oxonol V is not shown because of its similarity to those for oxonol VI.

modest effect of these probes on the main phase transition enthalpy change, the percentage reduction of the pretransition ΔH is large. When present at 1 mol%, all of the probes reduce this ΔH to almost one half that for the pure lipid suspension. A monotonical decrease in ΔH is seen for merocyanine 540 and oxonol VI. There were, however, no apparent trends in the plots of the pretransition cooperative units vs. mol% probe, the dyes having little or no effect on the cooperativity of the pretransition up to 3 mol%.

Sturtevant [23] and Albon and Sturtevant [24] have recently shown, at least in principle, that the excess heat capacity curves for the lipid bilayers (with impurities present) near the gel-to-liquid crystal phase transition can be represented by an equation derived from the ideal solution theory. In the case of the melting of the hydrocarbon chains, (all-*trans*, linear configuration to a disordered *gauche* and *trans* state), the impurities (dyes in our study) most probably will distribute between the two phases; thus, a distribution coefficient must be included in the analysis. When this is done, the equation relating temperature (T) to fraction (α) of lipid molecules melted is

$$T/T_0 = 1 - RT_0[(1/\Delta H_{vH})\ln\{(1-\alpha)/\alpha\} + (\ln X_1/\Delta H_{cal})(1/(K/(1-K)+\alpha))] \quad (3)$$

in which ΔH_{vH} and ΔH_{cal}, respectively, are the van 't Hoff and calorimetric enthalpy change for the transition, T_0 is the temperature at the transition midpoint for pure lipid bilayers, K is the distribution coefficient for the impurities between phases ($K = X(\text{gel})/X(\text{liquid crystal})$), and X_1 is the mole fraction of the lipid in the suspensions. For a two-state transition between a gel and a liquid crystal phase, the excess heat capacity is related to the derivative of α with respect to T

$$C_{ex} = (\Delta H_{cal})(d\alpha/dT) \quad (4)$$

Combining this relationship with the derivative

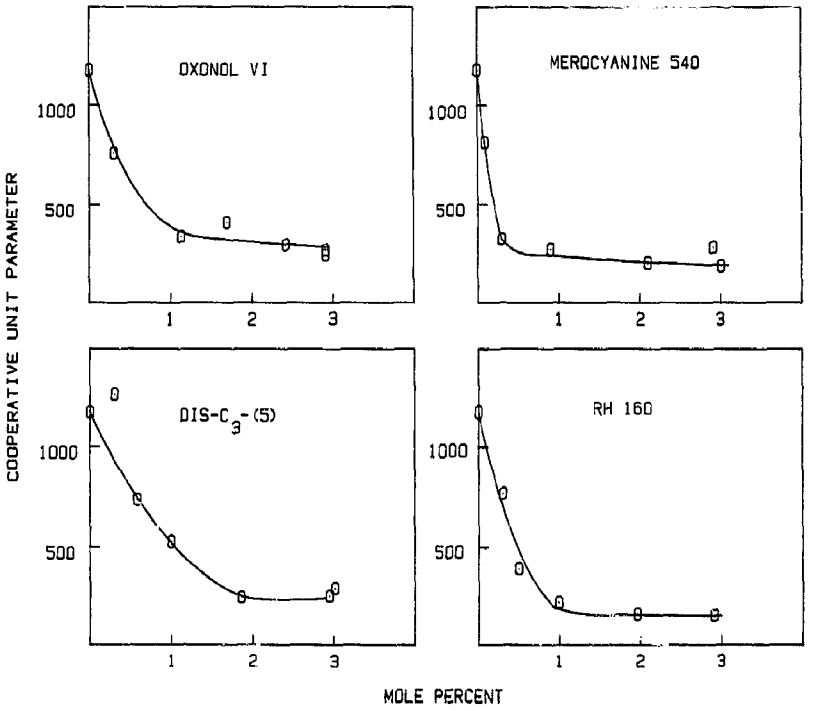

Fig. 4. CUP for the main transition plotted versus mol% of probes in DMPC suspensions. Data for oxonol V are similar to those for oxonol VI and are not shown.

derived from Eqn. 3 yields the equation for C_{ex} as a function of temperature and α

$$C_{ex} = [\Delta H_{cal}\Delta H_{vH}/RT^2]\left[1/\left\{(1/(1-\alpha)\alpha) - (\Delta H_{vH} \ln X_1/\Delta H_{cal})(1/(K/(1-K)+\alpha)^2)\right\}\right] \quad (5)$$

For any particular temperature, Eqn. 3 can be solved numerically for α which can then be used in Eqn. 5 to calculate C_{ex} for any set of parameters. Variation of these parameters via a non-linear least-squares procedure provides the set of parameters which can be used in Eqns. 3–5 to give the best fit for the experimental data. Sturtevant [23] reported that he was unable to fit the wings of the C_{ex} data for DMPC with the above equation, but he did not state explicitly his numerical procedure. Simply calculating T from Eqn. 3 at uniform increments of α and calculating the derivative from this data produces curves that do not fit the experimental data in the wings. Using the analytical expression for the derivative derived from Eqn. 3 yields curves that fit synthetic and experimental profiles quite well over the entire temperature range, even at mol% > 3. This model, as Sturtevant [25] has recently shown, is only strictly valid for water-insoluble compounds or those with very high affinities for the lipid phase; both criteria, as is shown in the discussion, appear to be met by the dyes in this study.

The best fit for any of our data is shown in panel A of Fig. 7, in which the actual data are represented by the symbols and the calculated profile is the solid line. Somewhat less satisfying fits were found for some suspensions, and the worst fit is shown in panel B, Fig. 7. All other fits were between these two cases. In all cases, T_m values derived for the pure lipid by the non-linear least-squares procedure are within 0.05°C of 24.40°C determined from the profile of pure DMPC suspensions; ΔH_{cal} values taken from the integration of the actual C_{ex} profiles are close to

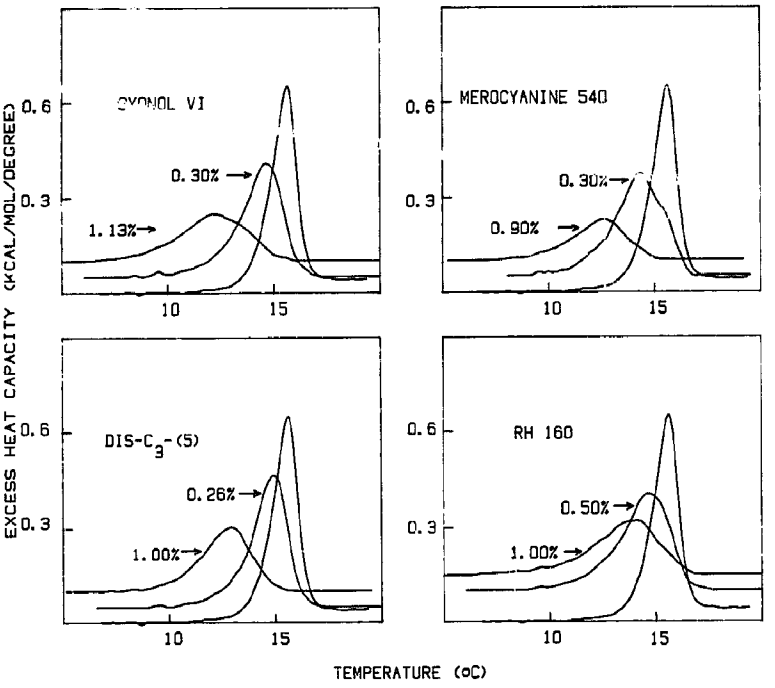

Fig. 5. The effect of the four types of potential-sensitive probe on the excess heat capacity profile of the DMPC preparation pretransition. The narrowest heat capacity profile in each panel is that for the dye-free DMPC suspension.

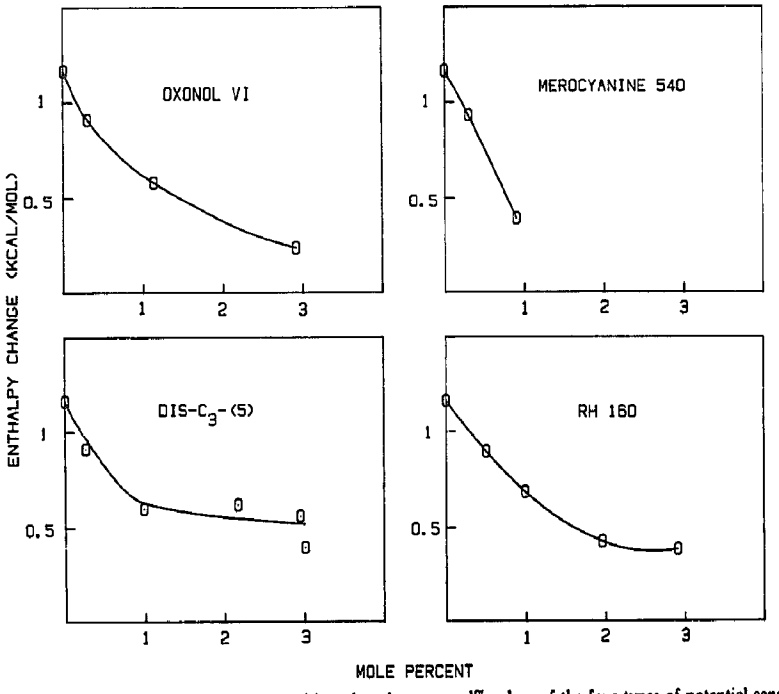

Fig. 6. Calorimetric enthalpy change for the pretransition plotted versus mol% values of the four types of potential-sensitive probe employed in this investigation. The lines are the best fits to the data.

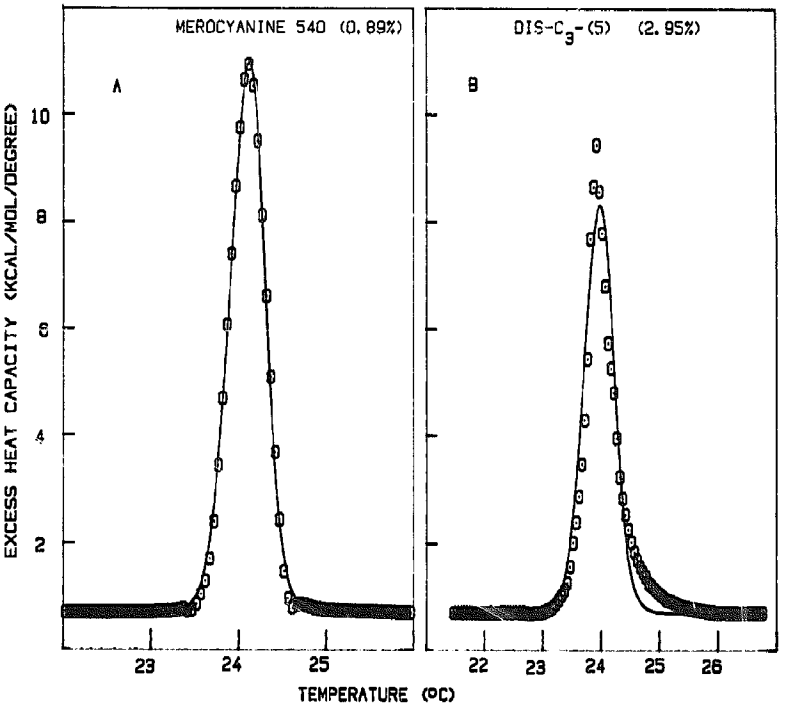

Fig. 7. Two comparisons of the ideal solution theory curves with the actual heat capacity profiles for the main phase transition in a DMPC multilamellar preparation. The solid lines were generated with the theoretical analysis based on the ideal solution theory (see text), and the symbols are data points. The parameters used in the fits are: for merocyanine 540 (panel A, best fit found) $X_1 = 0.991$, $\Delta H_{cal} = 5.21$ kcal/mol, $\Delta H_{vH} = 1876$ kcal/mol, $T_0 = 297.46°C$, and $K = 0.5$; for diS-C_3-(5) (panel B, worst fit) $X_1 = 0.971$, $\Delta H_{cal} = 4.94$ kcal/mol, $\Delta H_{vH} = 1433$ kcal/mol, $T_0 = 297.53°C$, and $K = 0.67$.

those from the fitting procedure; and the ΔH_{vH} values are always higher than those from the calorimetric procedure.

When the experiments on the multilamellar suspension were extended to higher mol% values (Fig. 8), a number of surprising results were obtained. First, even up to 12 mol%, the profile for a suspension with diS-C_3-(5) present could be reproduced by the ideal solution theory. Each of the other probes first caused the profiles to be asymmetric, and at higher levels, the profiles for oxonol V and merocyanine 540 consisted of more than one peak. For the suspension with 24 mol% oxonol VI, the profile is spread from 0°C to 30°C, and merocyanine 540 in contrast to the other probes causes a portion of the profile to appear above 30°C.

In the initial stages of our investigations, we attempted studies with unilamellar vesicles with diameters near 300 Å. The excess heat capacity profiles for such preparations are both broad and complex (see panel A, Fig. 9); however, this pattern transforms spontaneously, over a 2–3 day period at room temperature, into one similar to that reported in the literature for large vesicles [21], and is apparently due to a fusion of small vesicles into larger ones [11]. The same effect occurred in a much shorter period when diS-C_3-(5) was present: the profile immediately started to sharpen and, after 6 h, the profile consisted of a well-defined pretransition approx. 10°C below the gel-to-liquid crystal transition signal (panel C, Fig. 9). Nevertheless, the gel-to-liquid crystal transition of suspensions formed by aging the sonicated preparation is much broader, even in the absence of the dye, than those observed for the vortexed suspension which are multilamellar. Also, the peak for this transition with a probe present is clearly

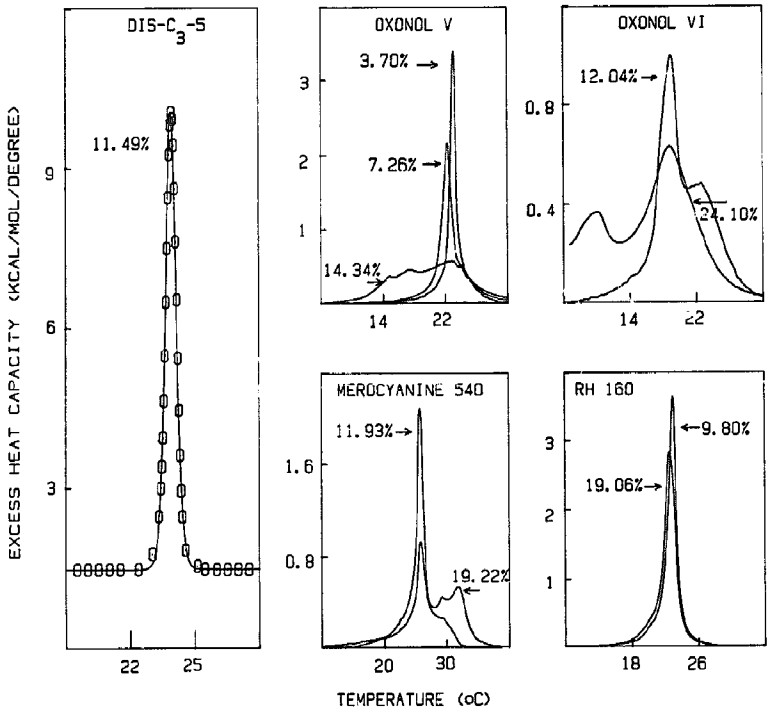

Fig. 8. Representative heat capacity profiles for DMPC suspensions with high mol% of the probes present. A comparison of the ideal solution theory curve with the actual data is shown for diS-C_3-(5) at 11.49 mol% (parameters obtained from the fitting procedure were: $\Delta H_{cal} = 5.42$ kcal/mol, $\Delta H_{vH} = 1173$ kcal/mol, $T_0 = 297.49$, $X_1 = 0.858$, and $K = 0.91$). For each of the other probes, profiles are given at intermediate and much higher mol% values.

bimodal, (see the inset in panel C, Fig. 9) which could be due to a distribution of the dye between the inside and outside layers of the vesicles.

Discussion

Each of the probes included in this study is known to bind to unilamellar vesicles [21], and one assumes that the Langmuir isotherm constant for this type of liposome is not much different than would be observed for the suspension in this study. Using these constants, we calculate that less than 1% (0.14% oxonol V, 0.66% oxonol VI, 0.09% merocyanine 540, 0.41% diS-C_3-(5) at a formal molarity of the dye of $3.7 \cdot 10^{-5}$ M) of each of the probes is in the aqueous phase up to 5 mol%, and the percentage bound does not vary appreciably over the 20°C temperature range of this study. Thus, neither the concentration dependence of the parameters found at low levels for each probe nor the differences found between probes can be ascribed to significant variations in the fraction of the probes associated with the lipid suspensions. At higher levels, larger amounts may be present in the aqueous phase, but their concentrations will not exceed the solubility limits, which are estimated to be in the 10^{-5} to 10^{-6} M range. Whatever the actual value is for the aqueous concentration of the dye, it is exceedingly small and constant in the temperature range of the experiment. Furthermore, the mole fraction of solute in the lipid phase is constant, and this is what is required for application of the ideal solution theory.

Sturtevant [23] found the model used in our curve-fitting procedure to be valid for the simple, non-soluble solutes, hexadecane and dodecane, which are not expected, on theoretical grounds, to form stable complexes with individual lipid molecules or disrupt the lipid bilayer at low mol%

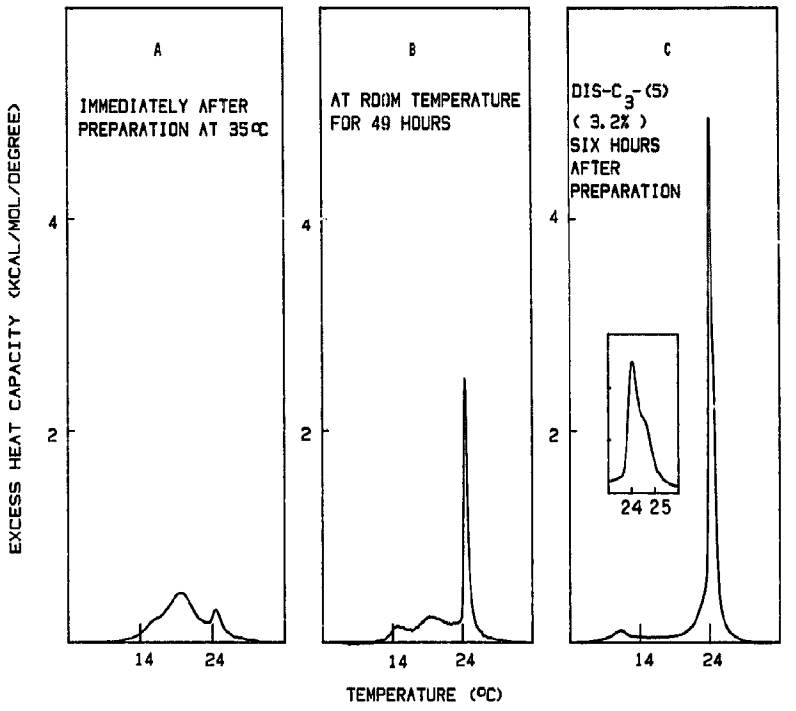

Fig. 9. The effect of diS-C_3-(5) on the phase transition properties of small unilamellar DMPC vesicles prepared by a sonication procedure. Panel A is the excess heat capacity profile of the dye-free vesicles and panel B is that of the dye-free vesicles after 49 h. Panel C is the excess heat capacity profile for vesicles after 6 h in the presence of the dye at 3.2 mol%. A pretransition and a markedly narrowed peak near the main phase transition are readily observable; however, the latter profile still has a high temperature shoulder, as illustrated in the inset in panel C.

values. For all the solutes in this study, the least-squares program based on this model produced excellent fits at mol% < 4; thus, our results are consistent with the conclusion that the probes form approximately ideal or at least regular solutions in both the gel and liquid crystal phases. The distribution between the two phases slightly favors the liquid crystal phase, i.e., the distribution coefficient (X(gel)/X(liquid crystal)) is near 0.6 for all probes. Deviations from this model at higher levels are seen for all probes except diS-C_3-(5), and this pattern is similar to the results reported by Lelkes et al. [26] for merocyanine 540 in dipalmitoyllecitin suspensions. At least two peaks are seen for oxonols V and VI and merocyanine 540 at mol% > 10, and these effects maybe due to lateral phase separation between two different domains caused by the presence of the probes, as has been suggested by Lelkes et al. [26] for the behavior of DPPC bilayers with merocyanine 540 present. Even at very high mol% values, diS-C_3-(5) causes changes in the DSC profiles that are completely consistent with the ideal solution model. Furthermore, ΔH_{cal} for DMPC with 11.7 mol% present is 5560 cal/mol, which is within experimental error the same as ΔH^0_{cal}. Both these observations, coupled with the marked enhancement of the fusion of vesicles by this probe prompt us to conclude that diS-C_3-(5) does not strongly interact with the lipid molecules in the bilayer, which is consistent with the probe weakly interacting with the lipid surface. Such an interaction should produce partial molal enthalpies for the probe in each phase that are almost the same, and ΔH_{cal} for the transition found for the pure lipid suspensions will be exactly the same as that found for diS-C_3-(5).

When this is not the case, the ΔH_{cal} based on the mole fractions of lipid molecules present should be approximately

$$\Delta H_{cal} = \Delta H^0 \text{cal} + [(1 - X_1)/X_1]\Delta H_{trans} \quad (6)$$

in which ΔH^0_{cal} is the enthalpy change for the transition for the pure lipid suspension and ΔH_{trans} is the enthalpy change for the transfer of the solute between the two types of lipid phase. In our studies, the ratio $(1 - X_1)/X_1$ is in the 0.01–0.30 range; thus, the observed downward trend in ΔH_{cal} found for all probes except diS-C_3-(5), either from the curve-fitting program or the area under the curve, is due to a negative ΔH_{trans} of −17, −20 and −47 kcal/mol for merocyanine 540, RH 160 and oxonol VI, respectively. Combining these values with the equilibrium constants derived from the fitting procedure, entropy changes for this process, ΔS_{trans}, are −55, −66 and −155 cal/mol per K for merocyanine 540, RH 160 and oxonol VI, respectively. Katz and Diamond [27–30] have studied the distribution of several simple solutes between the aqueous and lipid phases, and these data have been used to determine ΔH_{trans} (kcal/mol) and ΔS_{trans} (cal/mol per K) to be −20.7 and −69 for butyramide; −24.5 and −85 for ethyl acetate, and approx. −24 and −79 for acetone. These parameters are in the same range found in this study from the analysis of the DSC profiles.

In the gel state the rigidity of the hydrocarbon chains probably causes the solutes to be near the glycerol backbone or on the surface of the bilayer, unless the solute can form a well-defined complex with the hydrocarbon chains, as is thought to be the case for cholesterol [31]. Once the hydrocarbon chains are disordered, the solute can adopt conformations that are lower in potential energy and nearer the hydrocarbon chains, and this is probably why the calculated ΔH_{trans} and ΔS_{trans} are negative for three types of the probe. From these observations and analyses alone, we conclude that all probes employed in this study are probably only weakly attached to the surface or headgroup area of the bilayer in the gel phase and may interfere with the solvation of the headgroups in this phase. Above the transition temperature, the probes can penetrate the open spaces in the hydrocarbon region caused by an increase in the number of *gauche* conformations, and may on average be associated, to some extent, with this region. Oxonol V, for example, is unable to cross the bilayer of dipalmitoylphosphatidylcholine vesicles at temperatures below that of the gel-to-liquid crystal transition, but readily permeates the vesicle bilayer when it is in the latter fluid phase [32].

Our results for merocyanine 540 are not entirely in agreement with those of Lelkes et al. [26], who studied the effect of this probe on the main phase transition of DPPC. At mol% > 3, they found two closely spaced peaks in the excess heat capacity curves. Only a shoulder appeared at 3 mol%, whereas two peaks of almost equal height appeared at 33 mol%, one of which was centered virtually at the T_m of the transition for DPPC. These results may not be directly comparable to our work, because we used lipid concentrations in the 3 mg/ml range, which is a factor of 35 less than those used by these investigators. In our experiments, the excess heat capacity curves were virtually flat at 5 mol% dye and 2 mg/ml of lipid, whereas Lelkes et al. observed peaks in the DSC profile which were similar in magnitude to that for pure DPPC at values up to 33 mol% merocyanine 540. The very small residual excess heat capacity profile for DMPC with merocyanine 540 present at higher levels (see Fig. 8) does have a shoulder, but this is at a temperature above T_m for pure DMPC. At 19 mol% the DSC profile has several well-defined peaks in the 20–35°C range. If we interpret these results along the lines suggested by Lelkes et al. [26], multiple phases are forming at the higher probe levels. Jain and Wu [33] found the profiles of DMPC with an antibiotic present to be drastically different from those for DPPC and the same antibiotic. A complex pattern occurred for DMPC, but this was not the case for DPPC. Presumably this type of differentiation is responsible for the variance found between the two results for merocyanine 540. If the two peaks in the DPPC/merocyanine 540 system and those at higher levels for the DMPC/merocyanine 540 system are due to the existence of more than one gel phase, this could be caused by limited ideal solubility of merocyanine 540 in DPPC as well as in DMPC.

Several other workers have performed DSC measurements on lipids in the presence of drugs and hydrophobic molecules, and these have recently been reviewed by Bach [34]. Unfortunately, many of the studies were performed at high mol% values and are not directly comparable to the data

gathered by us in the range 0–5 mol%. Nevertheless, certain patterns have been recognized in the more than 100 compounds studied by Jain and Wu [33], who have classified the effects on the basis of the most probable location of the probes in the bilayer. All of the probes except diS-C_3-(5) cause the residual profiles to split eventually into more than one peak. This observation, coupled with the substantial broadening caused by these probes places them in a type A classification, which in the Jain and Wu scheme is a characteristic of molecules associated with the C-2 to C-8 region. Again, we conclude that diS-C_3-(5) does not penetrate this far into the bilayer because its profiles, at all concentrations, are typical of compounds assigned by Jain and Wu as near the headgroups of backbone or, alternatively, it could be between the two layers, but this does not seem likely for a charged moiety and is not consistent with the rapid fusion of vesicles in the presence of diS-C_3-(5).

In pure lipid preparations, the pretransition is thought to be due in part to a change in the lipid fatty acid packing from a disordered orthorhombic geometry to a hexagonal array [35]. Additional contributions from reorientations of the headgroup during this transition cannot be excluded and, to the extent that the headgroups do contribute to the pretransition, the probes employed in this study do have locations that embrace this bilayer domain as judged from the rather large effects of the dyes on the pretransition enthalpy. Oxonols V and VI and merocyanine 540 appear both to affect strongly the enthalpy (Fig. 6), an observation that suggests the perturbation of the former probes, and to a lesser degree that of RH 160 and diS-C_3-(5) as well, extends well into the headgroup region, and hence they behave partially as perturbants that are located at the bilayer surface and interact with the phosphatidylcholine headgroup [33].

Jain and Wu [33] suggested that the size of the cooperative unit is largely governed by interactions of the acyl chain groups in the C-1 to C-10 region. The prominent decrease in the cooperativity parameter caused by the potential-sensitive probes employed in these investigations, particularly the sharp decrease for all except diS-C_3-(5), suggests that the perturbation of the dyes on bilayer structure extends into the C-1 to C-9 region. The question, however, arises of why the presence of the probes at less than one mol% drastically decreases the cooperativity parameter; the latter effect is particularly pronounced in the case of the merocyanine 540 and RH 160 probes (Fig. 4). If one views this result from the prospective of the Fisher cluster model which was applied to the main transition by Tsong and associates [17], the probes were clearly very effective in reducing the average size for the clusters in the melted bilayers. Although strong interactions between the probes and the lipid molecules are not necessary for such an effect, an exact mechanism for this effect is not immediately obvious.

Acknowledgments

These investigations were supported by NIH award GM30552 and by NSF equipment grant DMB-8500319.

References

1 Bashford, C.L. (1981) Biosci. Rep. 1, 183.
2 Bashford, C.L. and Smith, J.C. (1979) Methods Enzymol. 55, 569–586, Academic Press, New York.
3 Cohen, L.B. and Salzberg, B.M. (1978) Rev. Physiol. Biochem. Pharmacol. 83, 35–88.
4 Waggoner, A.S. (1979) Annu. Rev. Biophys. Bioeng. 8, 47–68.
5 Waggoner, A.S. (1976) J. Membr. Biol. 27, 317–334.
6 Smith, J.C. (1987) in Spectroscopic Membrane Probes (Loew, L.M., ed.), Vol. 2, pp. 153–197, CRC Press, Boca Raton.
7 Silver, B.L. (1985) The Physical Chemistry of Membranes, The Solomon Press, New York.
8 Cevc, G. and Marsh, D. (1987) Phospholipid Bilayers, Physical Principles and Models, John Wiley & Sons, New York.
9 Marbey-Gaud, S. (1981) in Liposomes from Physical Structure to Therapeutic Applications (Knight, C.G., ed.), pp. 105–133, Elsevier/North-Holland Biomedical Press, Amsterdam.
10 McElhaney, R.N. (1982) Chem. Phys. Lipids 30, 229–259.
11 Bammel, B.P., Brand, J.A., Simmons, R.B., Evans, D. and Smith, J.C. (1987) Biochim. Biophys. Acta 896, 136–152.
12 Smith, J.C., Russ, P., Cooperman, B.S. and Chance, B. (1976) Biochemistry 15, 5094.
13 Privalov, P.L. (1980) in Biological Microcalorimetry (Beezer, T., ed.), pp. 413–453, Academic Press, New York.
14 Biltonen, R.L. and Freire, E. (1978) CRC Crit. Rev. Biochem. 5, 85–124.

15 Thompson, L.K., Sturtevant, J.M. and Brudvig, G.W. (1986) Biochemistry 25, 6161–6169.
16 Zimm, B.H. and Bragg, J.K. (1959) J. Chem. Phys. 31, 526–535.
17 Kanehisa, M.I. and Tsong, T.Y. (1978) J. Am. Chem. Soc. 100, 424–432.
18 Heinonen, J.R. and Lahti, R.J. (1981) Anal. Biochem. 113, 313–317.
19 Dufour, J., Nunnally, R., Buhle, L. and Tsong, T.Y. (1981) Biochemistry 20, 5576–5586.
20 Lentz, B.R., Friere, E. and Biltonen, R.L. (1978) Biochemistry 17, 4475–4480.
21 Parente, R.A. and Lentz, B.R. (1984) Biochemistry 23, 2353–2362.
22 Mabrey, S. and Sturtevant, J.M. (1976) Proc. Natl. Acad. Sci. USA 73, 3862–3866.
23 Sturtevant, J.M. (1982) Proc. Natl. Acad. Sci. USA 79, 3963–3967.
24 Albon, N. and Sturtevant, J.M. (1978) Proc. Natl. Acad. Sci. USA 75, 2258–2260.
25 Sturtevant, J.M. (1984) Proc. Natl. Acad. Sci. USA 81, 1398–1400.
26 Lelkes, P.I., Bach, D. and Miller, I.R. (1980) J. Membr. Biol. 54, 141–148.
27 Katz, Y. and Diamond, J.H. (1974) J. Membr. Biol. 17, 69–86.
28 Katz, Y. and Diamond, J.H. (1974) J. Membr. Biol. 17, 87–100.
29 Katz, Y. and Diamond, J.H. (1974) J. Membr. Biol. 17, 101–120.
30 Katz, Y. and Diamond, J.H. (1974) J. Membr. Biol. 17, 121–154.
31 Genz, A., Holzwarth, J.F. and Tsong, T.Y. (1986) Biophys. J. 50, 1043–1051.
32 Bashford, C.L., Chance, B., Smith, J.C. and Yoshida, T. (1979) Biophys. J. 25, 63–80.
33 Jain, M.K. and Wu, N.M. (1977) J. Membr. Biol. 34, 157–201.
34 Bach, D. (1983) in Biomembrane Structure and Function (Chapman, D., ed.), pp. 1–41, Macmillan Press, London.
35 Small, D.M. (1986) in Physical Chemistry of Lipids, (Small, D.M. ed.), pp. 475–522, Plenum Press, New York.